Evolution of the Angular Distribution of Laser-Generated Fast Electrons due to Resistive Self-Collimation

A.P.L.Robinson[1, a)] and H.Schmitz[1]
Central Laser Facility, STFC Rutherford-Appleton Laboratory,Didcot, OX11 0QX, United Kingdom

The evolution of the angular distribution of laser-generated fast electrons propagating in dense plasmas is studied by 3D numerical simulations. As resistively-generated magnetic fields can strongly influence and even pinch the fast electron beam, the question of the effect on the angular distribution is of considerable interest. It was conjectured that in the limit of strong collimation, there will only be minimal changes to the angular distribution, whereas the largest reduction in the angular distribution will occur where there is only modest pinching of the fast electron beam and the beam is able to expand considerably. The results of the numerical simulations vindicate this conjecture.

I. INTRODUCTION

This paper is concerned with the evolution of the angular distribution function of super-thermal relativistic electrons[1–3] generated by ultra-intense ($I\lambda^2 > 10^{18}\mathrm{Wcm}^{-2}\mu\mathrm{m}^2$) laser irradiation of solids or dense plasmas, specifically the evolution as the beam undergoes magnetic pinching[4] that arises from the electric field that arises as a return current is drawn in response to the high current densities of these 'fast' electron beams[5]. Such laser-generated fast electron beams lead to the production of energetic protons[6,7] and ions as well as x-rays[8] and neutrons[9]. They are therefore important to a number of proposed applications of laser-solid interactions at such high intensities. Fast electrons are crucial to one conception of the Fast Ignition variant of Inertial Confinement Fusion[10,11]

Although these fast electrons are relatively collision free (provided Z is not too high), they can be strongly affected by resistively generated magnetic fields. This opens up both the possibility of controlling the beam or the beam undergoing collimation into a single beam, as well as the possibility of there being highly disruptive filamentation[12] of the beam. Developing an understanding of fast electron transport has thus been a matter of considerable concern to the high powered laser community[13].

The term 'collimation' has been frequently used in conjunction with what might otherwise be termed 'magnetic pinching' of fast electron beams[4,14–25]. It is important, however, to make distinction between a magnetic field restricting the transverse size of a fast electron beam, and a magnetic field reducing the angular spread (or distribution) of the fast electrons with respect to the propagation axis[26]. In the literature what is often meant is the former (pinching the beam in space), and little attention is paid to the latter (shrinking the distribution in momentum space).

It is important to consider the angular distribution, and in this paper we examine the effect that self-pinching (or self-collimation) has on the angular distribution of a fast electron beam in a homogeneous target. Note that this is self-collimation in *homogeneous targets*, and not the structured targets that have been considered in some of the authors recent work[27–31] (or indeed any other inhomogeneous scenarios[32]). We begin by arguing that strong self-pinching will tend to limit any reduction in the angular distribution of the fast electron beam, whereas weak self-pinching has greater potential for reducing the angular distribution of the fast electron beam. We present a set of 3D particle-based hybrid simulations which show precisely this trend which we expect on theoretical grounds. We thus conclude that resistive self-collimation in a homogeneous target can lead to a shrinking of the angular distribution, however this is strongest when the spatial pinching is not too strong and the beam is allowed to expand somewhat. When the beam is very strongly pinched the shrinking of the angular distribution can be as weak as it is when the beam experiences minimal pinching.

II. THEORY

One can develop arguments for how differing degrees of magnetic pinching will affect the change in the angular distribution of the fast electrons by considering a set of hypothetical scenarios. Let us start at the extreme case where ideal magnetic pinching is very quickly achieved. In this scenario we imagine that the fast electron flow produces a magnetic 'pipe' consisting of purely azimuthal magnetic field that peaks at nearly constant radius and has a nearly constant peak value. Suppose that this pipe lies parallel to the x-axis which is the primary target axis. The magnetic field is so strong that it easily confines all the fast electrons. However this means that when fast electrons propagate down this pipe they undergo essentially specular reflection from the strong magnetic walls of the 'pipe'. Thus the angle of any single electron with respect to the x-axis never really changes except for the very brief periods when it reflects from the 'pipe' walls. This implies that overall there is no change to the angular distribution of the injected fast electrons, and we can

[a)]Electronic mail: alex.robinson@stfc.ac.uk

thus only conclude that very strong collimation (assuming it does not reduce the beam radius below its initial value) will prevent any substantial shrinking of the angular distribution of the fast electrons. We illustrate this scenario in figure 1(a).

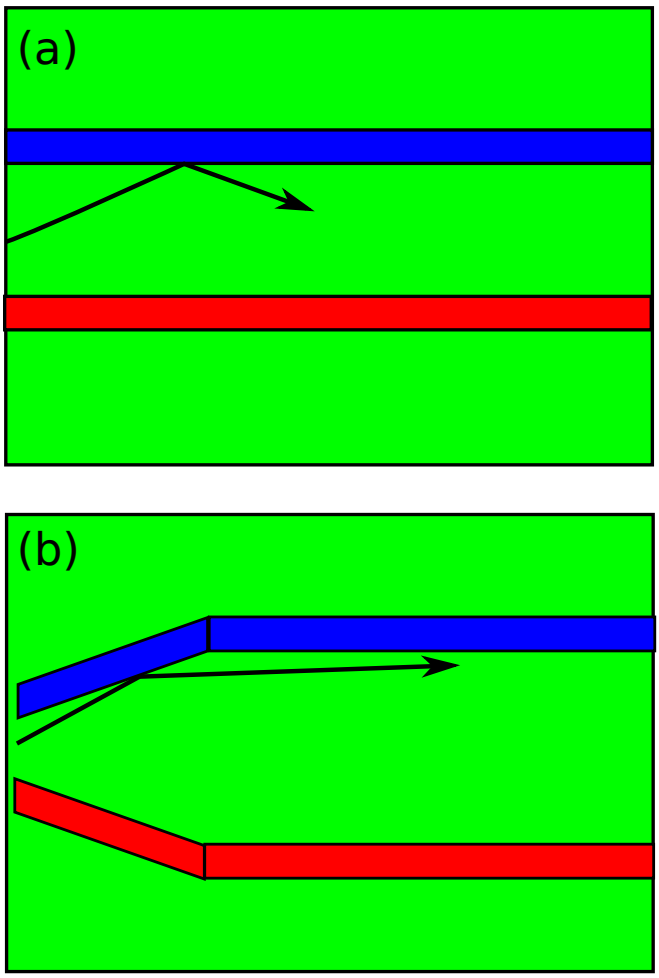

FIG. 1. Schematic illustration of (a) ideal magnetic pinching, where a straight magnetic pipe is rapidly formed, and (b) magnetic pinching where the beam radius first increases substantially before the beam radius is fixed. The x-axis, or primary target axis, is parallel to the horizontal axis in this picture.

Next we can consider the case where magnetic fields grow, but the beam radius increases steadily as the beam proceeds into the target. This scenario is illustrated in figure 1(b). In this regime magnetic pinching only restricts the rate at which the radius of the beam grows but does not ultimately 'clamp' the radius of the beam. In this case there will be a region of magnetic field which will look like a reflecting wall that is aligned at some angle, α, to the target axis. Here we can use a result obtained in previous studies[33] which considered oblique magnetic walls — a fast electron reflecting off such a wall will propagate at an angle,θ' to the target axis given by,

$$\theta' = \theta - 2\alpha, \tag{1}$$

where θ is angle to the target axis with which the fast electron is incident upon the wall. We therefore see that by allowing the beam to expand, the fast electrons can undergo reflections which can strongly reduce the angle with which they propagate with respect to the target axis.

In the case where magnetic fields grow very weakly, it can only be the case that not only will there be no magnetic pinching, but the reduction of the angular distribution will be highly limited as well. This brief, and mainly qualitative consideration of the expected cases therefore suggests the following hypothesis: as the degree of magnetic pinching becomes stronger one will see an increase in the reduction of the angular spread, however this must eventually reach an optimum point. Beyond this point the pinching will become strong and the reduction in the angular spread will progressively vanish. In the limit where the fast electron beam does not expand much beyond its initial radius, the fast electron angular distribution will be largely unaffected by the magnetic pinching.

This 'billiards' model of fast electrons, assumes, of course that the magnetic fields are always specularly reflecting the fast electrons. In order for specular reflection to occur the following condition must be satisfied[28],

$$B_\phi L_B > \frac{p_f}{e}\left(1 - \cos\theta\right), \tag{2}$$

where L_B is the characteristic thickness of the magnetic field, θ is the propagation angle of the fast electrons with respect to the target axis,p_f is the fast electron momentum, and B_ϕ is the characteristic magnitude of the azimuthal magnetic field. For any magnetic field that is resistively generated, given a Juttner-like distribution of electrons, there will likely be a significant fraction of the electrons that don't satisfy this condition. These unconfined electrons will always have their angle of propagation reduced somewhat as they escape through the magnetic fields. The total effect of growing stronger magnetic fields on the angular distribution will include the effect on both confined and unconfined fast electrons, and since the effect is different on each group it is difficult to make a simple estimation of what the actual trend will be. Some trends can be inferred however. If the resistivity is Spitzer-like then one expects the following scaling relation for the azimuthal magnetic field,

$$B_\phi \propto Z n_i^{3/5} j_f^{-1/5} t^{2/5} R^{-1}, \tag{3}$$

where R is the beam radius (see[4,5,28] for derivation of this relation). Furthermore one expects that $j_f = e\beta I_L/\varepsilon_f$ (β is the laser to fast electron conversion efficiency and ε_f is the mean fast electron energy). This scaling relation implies that increasing Z will tend to grow the magnetic

field, but the magnitude of the magnetic field does not vary strongly with laser intensity. Collimation is affected by the laser intensity through changes to the electron momenta in Eq. 2. There is also the additional complexity associated with the fact that the magnetic fields are both time-dependent and spatially inhomogeneous. This means that the distinction between 'confined' and 'unconfined' electrons cannot be determined by a single simple criterion.

There are therefore three important conclusions that we can come to from these main theoretical considerations. Firstly the problem posed in this paper is actually not a trivial problem as we hope the preceding discussion has made clear. Secondly, because of the complexity of the problem, it is important to address the problem numerically. Thirdly we can anticipate that in the limit where the majority of fast electrons are confined by the magnetic fields and well pinched that the angular distribution will be unchanged from the injection distribution which suggests that partial collimation of the fast electrons is actually better at reducing the angular distribution of the fast electrons. This suggests that over a wide range of conditions we should, despite the aforementioned complexity, observe a general trend in which the reduction of the angular distribution will become weaker and weaker as conditions move towards favouring strong pinching.

III. NUMERICAL SIMULATIONS

A. Set-Up

Simulations were performed using the 3D particle hybrid code ZEPHYROS. The 'standard' run used was set up as follows : A 200×200×200 grid was used with a 1μm cell size in each direction. The target was homogeneous in terms of composition (Z) and with a uniform density and initial temperature. We considered three different materials amongst all the simulations : pure CH_2, Al, and Ti. The simulations were either carried out with an initial temperature of 1 eV or 200 eV. The background resistivity was described by the model which closely follows Lee and More, but with the minimum electron mean free path taken to be $5r_s$, where r_s is the interatomic spacing. The background fluid equation of state was based on the Thomas-Fermi model (this includes the ionization state). The temporal profile of the injected fast electron beam is a top-hat function of τ_L =1 ps duration, and the transverse profile was a Gaussian with a characteristic radius of 5 μm radius which extended out to a 15 μm radius. The injected fast electron beam was chosen to model irradiation from I_L =1×10^{18}–10^{20}Wcm^{-2}, with the assumption of 30% conversion efficiency, and a laser wavelength of 1 μm. The fast electron angular distribution was chosen to be a $\cos^2\theta$ distribution throughout. Note that the axis this refers to is the x-axis of the simulation box, thus making the x-axis the main target axis (see Section II). The fast electron temperature used was set according to the Ponderomotive Scaling proposed by Wilks[1],

$$T_f = 0.511\left[\sqrt{1+\frac{I_L\lambda_L^2}{1.38\times10^{18}\mathrm{Wcm}^{-2}}}-1\right]\mathrm{MeV}. \quad (4)$$

Simulation	Intensity (Wcm^{-2})	Z	n_i (10^{28}m^{-3})	$T_{b,init}$ (eV)
A	10^{20}	2.66	12.9	200
B	10^{20}	13	6.0	200
C	10^{20}	22	15.6	200
D	10^{19}	2.66	12.9	200
E	10^{19}	13	6.0	200
F	10^{19}	22	15.6	200
G	10^{18}	2.66	12.9	200
H	10^{18}	13	6.0	200
I	10^{18}	22	15.6	200
J	10^{18}	2.66	12.9	1
K	10^{18}	13	6.0	1
L	10^{18}	22	15.6	1
M	10^{19}	2.66	12.9	1
N	10^{19}	13	6.0	1
O	10^{19}	22	15.6	1
P	10^{20}	2.66	12.9	1
Q	10^{20}	13	6.0	1
R	10^{20}	22	15.6	1
S	10^{19}	26	8.42	200
T	10^{19}	29	8.42	200

TABLE I. Table of Simulation Parameters

A total of twenty simulations were carried out, and they are labelled A–R. We have tabulated the details of each simulation in Table I. The aim of choosing the simulation parameters was to cover a wide range of conditions that ranged from favouring magnetic pinching (low intensity and high Z) through to conditions in which pinching would probably be minimal (high intensity and low Z). By measuring the degree of pinching (e.g. beam width) and the resulting average angular distribution we can then examine the link between magnetic pinching and the changes in the angular distribution of the fast electrons.

B. Results

The results of this study were analyzed in terms of the mean propagation angle of the fast electrons, and the beam width. The 'propagation angle' of the fast electrons refers to the 'polar angle' that a fast electron makes with respect to the x-axis (see Section II and), and thus the 'mean' propagation angle is angle obtained by taking the average over the entire fast electron population. The 'beam width' is a measure of the spatial extent of fast electron density perpendicular to the x-axis, and we define this in terms of the full width at half-maximum (FWHM) of the fast electron density perpendicular to the

x-axis. The beam width is constrained by the azimuthal magnetic field that develops, so the extent (or 'degree') to which the beam is magnetically pinched is related to the beam width. We thus use the beam width as a quantitative measure of magnetic pinching, and where a term such as 'degree of pinching' is employed, the quantitative measure is the beam width.

The principal results of this study are presented in figure 2 in which we show the change in the mean propagation angle with respect to the x-axis by 1 ps from the mean propagation angle of the injection distribution against the FWHM of the fast electron beam at x =25μm at 1 ps, i.e. we plot $\Delta\bar{\theta}$, where,

$$\Delta\bar{\theta} = \bar{\theta}_{inj} - \bar{\theta}_{sim}, \tag{5}$$

with $\bar{\theta}_{sim}$ being calculated from all fast electrons at 1 ps. Both the beam width and mean propagation angle plotted in figure 2 are instantaneous values or 'snapshots'. This quantity is then plotted against the FWHM of the fast electron beam at x =25μm at 1 ps which is obtained from the fast electron density outputs. As the injected angular distribution is a $\cos^2\theta$ distribution the mean angle at injection is $\bar{\theta}$ =38.19. Note that in all cases the mean angle was smaller than this,so $\Delta\bar{\theta}$ represents the magnitude of the *decrease* in $\bar{\theta}$.

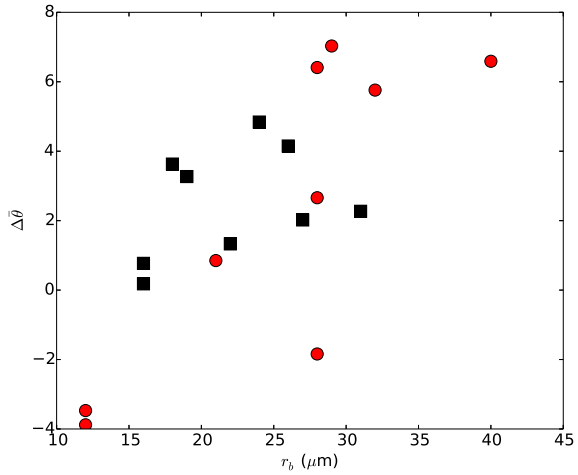

FIG. 2. Plot of change in mean propagation angle (with respect to x-axis) against full width a half maximum of the fast electron beam at x =25μm(all at 1 ps in time). Black squares are the results for runs A–I, and the red circles are those from runs J–R.

From figure 2 it can be seen that although there is no regular variation of $\Delta\bar{\theta}$ with the beam radius at this time there appears to be a general trend for $\Delta\bar{\theta}$ to increase with the beam radius. Since increased magnetic pinching means a decreased beam radius, what figure 2 therefore suggests is that weaker magnetic pinching leads to a stronger reduction in the angular distribution. This is entirely in line with the general thrust of our conjecture in Section II under the assumption that none of the simulations are in the regime where the magnetic field is very weak and that most fast electrons are well confined by the magnetic fields. Figure 2 (i.e. all of the results put together) appears to be inconsistent with the alternative hypothesis — that increasing magnetic pinching leads to a reduction in the angular distribution.

The high level of what might be termed 'scatter' in figure 2 indicates that there are some subtleties that should be considered. Suppose that we just plot the results (in the same fashion) for runs A–F, as well as runs P, Q, and R. These are shown in figure 3.

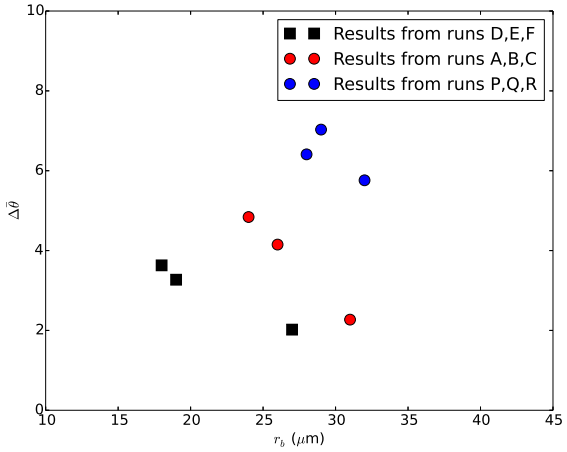

FIG. 3. Plot of change in mean propagation angle (with respect to x-axis) against full width a half maximum of the fast electron beam at x =25μm(all at 1 ps in time). Legend indicates which block of results each point belongs to.

In figure 3 the runs are grouped in blocks (A–C,D–G,P–R) where the laser intensity is constant and Z varies. This figure is very interesting, and an examination of it goes some way to dissecting the subtleties of figure 2. Suppose we look either of sets A–C or D–F in isolation. Just from those 3 points alone one might conclude that stronger collimation (lower beam width) leads to a greater reduction in $\bar{\theta}$. However we can re-plot this sub-set of the simulation results so that we re-group the results into groups where Z is constant. This is done in figure 4. This shows that if we now follow each Z group individually then we would conclude that increasing collimation leads to a decrease in $\bar{\theta}$ (as per our conjecture). Overall from the subset of the results shown in figures 3 and 4 it is hard to draw general conclusions about the relation between magnetic pinching and changes in the angular distribution of the fast electrons, but the trends that come from varying laser intensity and Z *separately* are much clearer.

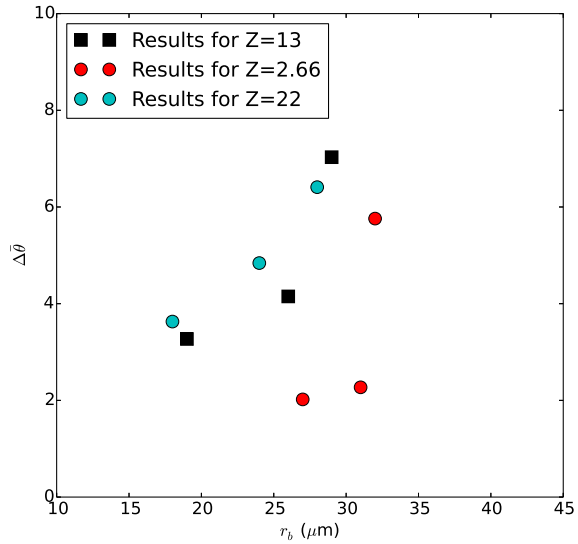

FIG. 4. Plot of change in mean propagation angle (with respect to x-axis) against full width a half maximum of the fast electron beam at x =25μm(all at 1 ps in time). Results are taken from runs A–F and P–R, and are grouped according to Z as indicated by the legend.

If we think about this in terms of the distinction between confined and unconfined electrons that we made in Section II then this can be explained. Specifically one must recall the points made in relation to Eq.s 2 and 3. When Z is increased, stronger magnetic fields are developed (linear scaling in Eq. 3), but the fast electron mean energy and momenta are unchanged (as I_L is held constant). While this will mean that some electrons move from being 'unconfined' to 'confined', it also means that *all* 'unconfined' electrons will experience a greater reduction in angle as they escape through the magnetic field. Therefore by increasing Z at constant I_L we might experience both increased collimation and a reduction in the angular distribution because of the effect on the unconfined fast electron population. In contrast if we decrease I_L and keep Z constant then we lower p_f which leads to increased confinement and collimation — while the magnetic field magnitude varies quite slowly (-1/5 power in Eq.3). While this does change the numbers in the confined and unconfined populations, it does mean that the majority of unconfined electrons will be only weakly affected because the change in the magnetic field will be small. Consequently we only see the effect of having more well-confined fast electrons, which means that we observe that the angular distribution is less and less changed as the degree of magnetic pinching increases. Ultimately the effect of increasing Z at a given intensity must lead to a large fraction of the fast electrons becoming confined and beyond this point the effect of increasing Z must be for the reduction in the angular spread to get smaller and smaller (we will now proceed to test this final point — see figure 5).

In order to carry out a further test of this analysis we have extended the set of D–F to include runs S and T. These additional runs are carried out under the same conditions as runs D–F but extend to higher Z. The results of this extended set (D–F,S & T) are shown in figure 5. This clearly shows that if we increase Z further eventually we find that the reduction in the mean angle reaches a maximum and declines thereafter.

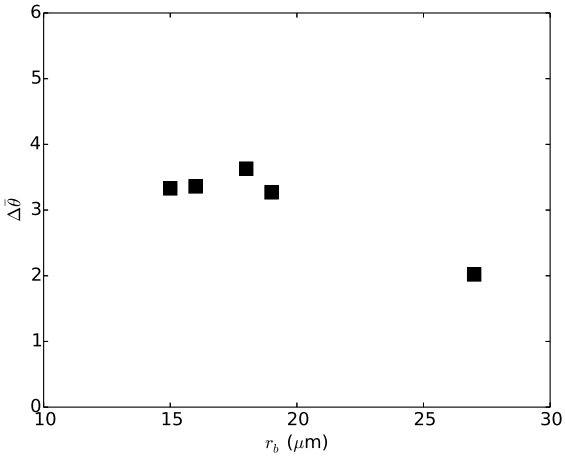

FIG. 5. Plot of change in mean propagation angle (with respect to x-axis) against full width a half maximum of the fast electron beam at x =25μm(all at 1 ps in time). Results are taken from runs D–F,S and T.

Directly showing the roles of 'confined' versus 'unconfined' electrons would require analysis of the full trajectory of each macroparticle in the simulation. Such a complex study will be a matter of future work. However there is further evidence for this distinction in the angular distributions obtained from these simulations. In figure 6 the angular distribution of the fast electrons at 2 ps in runs D–F, S, and T are plotted (the same runs as shown in figure 10). To complement this we also plot the maximum value of B_z at 1 ps in the simulation mid-plane in figure 7, as an indication of the magnetic field strength.

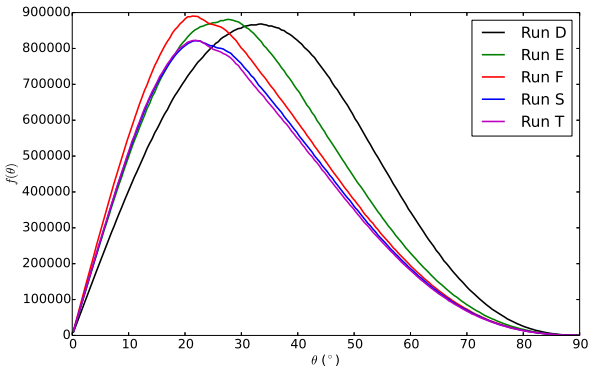

FIG. 6. Plot of angular distribution at 2 ps in runs D–F, S, and T as indicated.

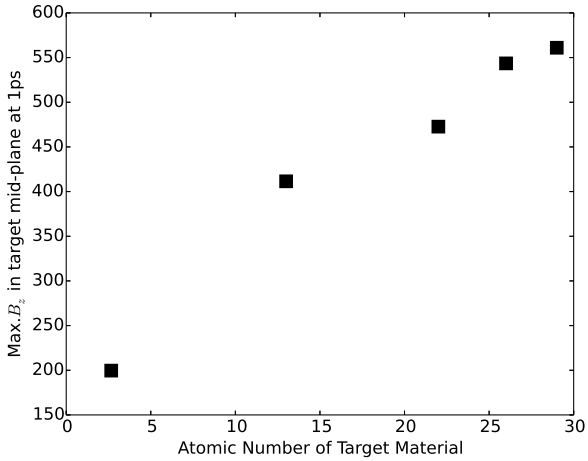

FIG. 7. Plot of maximum value of B_z in simulation mid-plane at 1 ps in runs D–F, S, and T (plotted as function of Atomic Number of target material).

Figure 7 shows that, on moving from simulation D to T in this sequence, the magnetic flux density grows without any apparent saturation. However figure 6 as well as 5 show that the changes to the angular distribution clearly do saturate on progressing through this sequence. Figure 5 shows this occurs in terms of the mean propagation angle. In figure 6 we see what happens in terms of the polar angular distribution, and we find that the angular distributions of runs S and T almost overlay one another. This is in sharp contrast to runs D–F which show the angular distribution undergoing progressive shrinking on proceeding from run D to run F (which agrees with what happens to the mean propagation angle). Despite the magnetic field continuing to become stronger, the effect on the angular distribution in runs S and T would appear to stop growing. These complemenatary figures are therefore evidence for fast electrons becoming confined, as once this occurs the fast electron angular distribution will not shrink any further. Further confirmation of this would require analysis of individual trajectories, which will have to be a matter for future work.

C. Tests of Sensitivity to Model Parameters

Given the complex behaviour exhibited by runs A–T, it is important to examine how sensitive our findings are to particular choices in the model and its parameters. To this end, runs A–G were repeated three times, each with a variation in the model. In the first batch of new runs (labelled A2–G2), the angular distribution of the injected fast electrons was changed from a $\cos^2\theta$ distribution to a uniform distribution up to a half-angle of 50°. In the second batch (labelled A3–G3), the radial profile of the injected beam was changed from a Gaussian to an exponential profile. In the third batch (labelled A4–G4), the fast electron scaling law was changed from the ponderomotive scaling (Eq. 4) to a Beg-like scaling law,

$$T_f = 0.3\left[\frac{I\lambda^2}{10^{18}\mathrm{Wcm}^{-2}\mu\mathrm{m}^2}\right]\mathrm{MeV}. \qquad (6)$$

Otherwise the same parameters as used in runs A–G to were used in these simulations. The results of these simulations are summarized in figures 8–10.

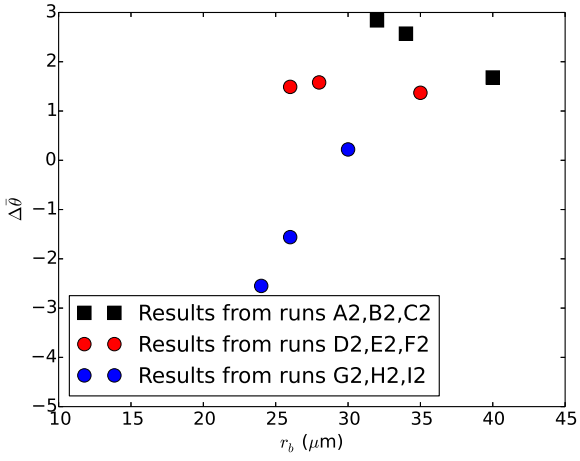

FIG. 8. Plot of change in mean propagation angle (with respect to x-axis) against full width a half maximum of the fast electron beam at x =25μm(all at 1 ps in time). Results are taken from runs A2–I2.

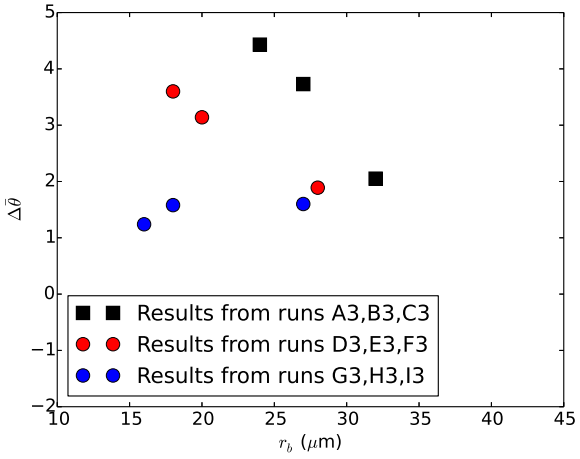

FIG. 9. Plot of change in mean propagation angle (with respect to x-axis) against full width a half maximum of the fast electron beam at x =25μm(all at 1 ps in time). Results are taken from runs A3–I3.

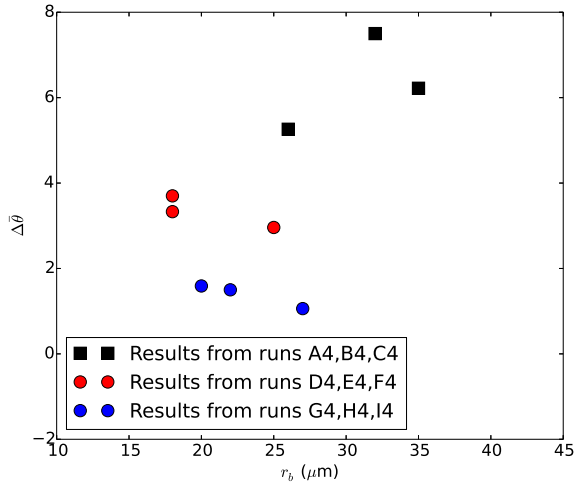

FIG. 10. Plot of change in mean propagation angle (with respect to x-axis) against full width a half maximum of the fast electron beam at x =25μm(all at 1 ps in time). Results are taken from runs A4–I4.

On examining figures 8–10 we can make two observations. Firstly we see that all three plots uphold the primary conclusion reached from runs A–T, namely that there is a global trend for increasing collimation (lower beam width) to lead to a smaller and smaller reduction in the angular distribution (the largest reduction in angular distribution occurs either at intermediate or maximum beam width). Secondly some of the complex trends in the data observed in runs A–T recur in the new sets. For example, it can be seen that on keeping I_L constant and increasing that $\Delta\bar{\theta}$ will rise with decreasing r_b in a number of sub-sets (A2–C2, A3–C3,D3–F3) which indicates that the phenomena associated with the effect of increased magnetic fields on the unconfined fast electrons not only recurs in these new simulation sets, but that it is quite a general phenomenon that is not peculiar to a particular choice of model parameters. Overall the new simulation results indicate that the conclusions drawn from runs A–T are quite general and are not a result of specific details of the numerical model.

IV. CONCLUSIONS

In this paper we have analysed the effect that magnetic pinching has on the angular distribution of fast electrons. Both theoretical considerations and numerical simulations indicate that it is important to distinguish between electrons that are confined and unconfined by the resistively generated magnetic fields. Unconfined electrons will always have their angular distribution reduced by increases in magnetic field, whereas well confined electrons will eventually experience no reduction in magnetic field once magnetic pinching is so strong that the beam radius is comparable to the laser spot size. Changes in the angular distribution with the degree of magnetic pinching therefore depend on how this is achieved and the relative split into the two sub-populations. When more magnetic pinching is induced by increasing Z the increased magnetic fields will collimate the unconfined electrons to a greater degree which means that the angular distribution can be reduced overall as there is stronger magnetic pinching. On the other hand, if stronger magnetic pinching is produced by reducing the laser intensity (which lowers the fast electron energy, but the magnetic field tends to scale slowly with I_L) then there is only a negligible effect on the unconfined electrons, but the confined electrons will be pinched more strongly — leading to less reduction in the angular distribution with stronger pinching. Over a wide parameter space the global trend is for stronger pinching to lead to a smaller and smaller reduction in the angular distribution of the fast electrons — this means that large reductions in the angular distribution of the fast electrons cannot be achieved while at the same time one is strongly pinching the beam. On trying out some variations on the numerical model used, the same trends were observed (Section III C) which indicates that our findings are not highly sensitive to the particular numerical model that has been used, and that these findings are probably quite general.

ACKNOWLEDGMENTS

This work was supported by the European Research Council's STRUCMAGFAST grant (ERC-StG-2012). APLR and HS are grateful for the use of computing resources provided by STFC's Scientific Computing Department.

[1] S. C. Wilks, W. L. Kruer, M. Tabak, and A. B. Langdon, Phys. Rev. Lett. **69**, 1383 (1992), URL http://link.aps.org/doi/10.1103/PhysRevLett.69.1383.

[2] A.Kemp and L.Divol, Phys.Rev.Lett. **109**, 195005 (2012).

[3] A.J.Kemp, F.Fiuza, A.Debayle, T.Johzaki, W.B.Mori, P.K.Patel, Y.Sentoku, and L.O.Silva, Nucl. Fusion **54**, 054002 (2014).

[4] A.R.Bell and R.J.Kingham, Phys.Rev.Lett. **91**, 035003 (2003).

[5] A. R. Bell, A. P. L. Robinson, M. Sherlock, R. J. Kingham, and W. Rozmus, Plas. Phys. and Control. Fusion **48**, R37 (2006).

[6] P.McKenna, A.P.L.Robinson, D.Neely, M.P.Desjarlais, D.C.Carroll, M.N.Quinn, X.H.Yuan, C.M.Brenner, M.Burza, M.Coury, et al., Phys.Rev.Lett. **106**, 185004 (2011).

[7] T.Z.Esirkepov, S.V.Bulanov, K.Nishihara, T.Tajima, F.Pegoraro, V.S.Khoroshov, K.Mima, H.Daido, Y.Kato, Y.Kitagawa, et al., Phys.Rev.Lett. **89**, 175003 (2002).

[8] C.D.Chen, P.K.Patel, D.S.Hey, A.J.MacKinnon, M.H.Key, K.U.Akli, T.Bartal, F.N.Beg, S.Chawla, H.Chen, et al., Phys.Plasmas **16**, 082705 (2009).

[9] I.Pomerantz, E.McCary, A.R.Meadows, A.Arefiev, A.C.Bernstein, C.Chester, J.Cortez, M.E.Donovan, G.Dyer, E.W.Gaul, et al., Phys. Rev. Lett. **113**, 184801 (2014).

[10] M.Tabak, J.Hammer, M.E.Glinksy, W.L.Kruer, S.C.Wilks, J.Woodworth, E. Campbell, M.D.Perry, and R.J.Mason, Phys.Plasmas **1** (1994).

[11] M.Tabak, D.S.Clark, S.P.Hatchett, M.H.Key, B.F.Lasinski, R.A.Snavely, S.C.Wilks, R.P.J.Town, R.Stephens, E.M.Campbell, et al., Phys.Plasmas **12**, 057305 (2005).

[12] J.Fuchs, T.E.Cowan, P.Audebert, H.Ruhl, L.Gremillet, A.Kemp, M.Allen, A.Blazevic, J.-C.Gauthier, M.Geissel, et al., Phys.Rev. **91**, 255002 (2003).

[13] A.P.L.Robinson, D.J.Strozzi, J.R.Davies, L.Gremillet, J.J.Honrubia, T.Johzaki, R.J.Kingham, M.Sherlock, and A.A.Solodov, Nuclear Fusion **54**, 054003 (2014).

[14] Y.Sentoku, E.d'Humieres, L.Romagnani, P.Audebert, and J.Fuchs, Phys.Rev.Lett. **107**, 135005 (2011).

[15] S.Chawla, M.S.Wei, R.Mishra, K.U.Akli, C.D.Chen, H.S.McLean, A.Morace, P.K.Patel, H.Sawada, Y.Sentoku, et al., Phys.Rev.Lett. **110**, 025001 (2013).

[16] X.H.Yang, M.Borghesi, and A.P.L.Robinson, Phys.Plasmas **19**, 062702 (2012).

[17] P.Leblanc and Y.Sentoku, Phys.Rev.E **89**, 023109 (2014).

[18] D.A.MacLellan, D.C.Carroll, R.J.Gray, N.Booth, M.Burza, M.P.Desjarlais, F.Du, B.Gonzalez-Izquierdo, D.Neely, H.W.Powell, et al., Phys.Rev.Lett. **111**, 095001 (2013).

[19] D.A.MacLellan, D.C.Carroll, R.J.Gray, N.Booth, M.Burza, M.P.Desjarlais, F.Du, D.Neely, H.W.Powell, A.P.L.Robinson, et al., Phys.Rev.Lett. **113**, 185001 (2014).

[20] M.Tatarakis, J.R.Davies, P.Lee, P.A.Norreys, N.G.Kassapakis, F.N.Beg, A.R.Bell, M.G.Haines, and A.E.Dangor, Phys. Rev. Lett. **81**, 999 (1998).

[21] F.Perez, A.Debayle, J.Honrubia, M.Koenig, D.Batani, S.D.Baton, F.N.Beg, C.Benedtti, E.Brambrink, S.Chawla, et al., Phys.Rev.Lett. **107**, 065004 (2011).

[22] M. Storm, A. A. Solodov, J. F. Myatt, D. D. Meyerhofer, C. Stoeckl, C. Mileham, R. Betti, P. M. Nilson, T. C. Sangster, W. Theobald, et al., Phys.Rev.Lett. **102**, 235004 (2009).

[23] J.S.Green, V.M.Ovchinnikov, R.G.Evans, K.U.Akli, H.Azechi, F.N.Beg, C.Bellei, R.R.Freeman, H.Habara, R.Heathcote, et al., Phys.Rev.Lett. **100**, 015003 (2008).

[24] K.L.Lancaster, J.S.Green, D.S.Hey, K.U.Akli, J.R.Davies, R.J.Clarke, R.R.Freeman, H.Habara, M.H.Key, R.Kodama, et al., Phys.Rev.Lett. **98**, 125002 (2007).

[25] J.J.Honrubia and J. ter Vehn, Plasma Phys.Control.Fusion **51**, 014008 (2009).

[26] A.Debayle, J.J.Honrubia, E.d'Humieres, and V.T.Tikhonchuk, Phys. Rev. E **82**, 036405 (2010).

[27] A.P.L.Robinson and M.Sherlock, Phys.Plasmas **14**, 083105 (2007).

[28] A.P.L.Robinson, H.Schmitz, and J.Pasley, Phys.Plasmas **20**, 122701 (2013).

[29] A.P.L.Robinson and H.Schmitz, Phys.Plasmas **20**, 062704 (2013).

[30] S.Kar, A.P.L.Robinson, D.C.Carroll, O.Lundh, K.Markey, P.McKenna, P.Norreys, and M.Zepf, Phys.Rev.Lett. **102**, 055001 (2009).

[31] B.Ramakrishna, S.Kar, A.P.L.Robinson, D.J.Adams, K.Markey, M.N.Quinn, X.H.Yuan, P.McKenna, K.L.Lancaster, J.S.Green, et al., Phys.Rev.Lett. **105**, 135001 (2010).

[32] R. Kodama et al., Nature **432**, 1005 (2004).

[33] A.P.L.Robinson, H.Schmitz, J.S.Green, C.P.Ridgers, and N.Booth, Plasma Phys. and Control. Fusion **57**, 064004 (2015).